lation was then obtained for Q_u:

$$Q_u = \left(\omega_0 - \frac{\omega_m}{3}\right)\frac{\tau}{2} \tag{2}$$

where

τ = relaxation time

ω_0 = resonant angular frequency $= 2\pi \times$ resonant frequency in cycles per second

$\omega_m = \gamma_0 M_0 = \mu_0 g(e/2m) M_0 = 2\pi f_m$ = angular frequency corresponding to the magnetization, in which

μ_0 = intrinsic permeability of free space $= 1.256 \times 10^{-6}$ henries per meter

g = Landé g factor $\cong 2.00$ for electrons in most ferrites

e/m = ratio of charge, e, to mass, m, of electron $= 1.759 \times 10^{11}$ coulombs/kg

M_0 = saturation magnetization of ferrite, amperes per meter.

This new formula for Q_u given above predicts that a value of $Q_u = 0$ should occur at $\omega_0 = \omega_m/3$, thereafter increasing linearly with increasing frequency, provided that τ is independent of frequency. According to the equation for Q_u derived using the Lax formula, the variation of Q_u is described by a straight line which intersects the origin, $Q_u = 0$ at $f_0 = 0$. These two relations given by (1) and (2) are shown in Fig. 1 for the case $\tau = 2 \times 10^{-7}$. The only qualification that must be applied to these formulas is that the material must be fully magnetized. For a spherical shape this requires that the operating frequency should be somewhat greater than $\omega_0 = \omega_m/3 = \gamma_0 H_0$, since a sphere becomes unsaturated at biasing fields of this magnitude For single crystal yttrium-iron-garnet this "saturation frequency" occurs at $f_0 = f_m/3 = 1670$ Mc.

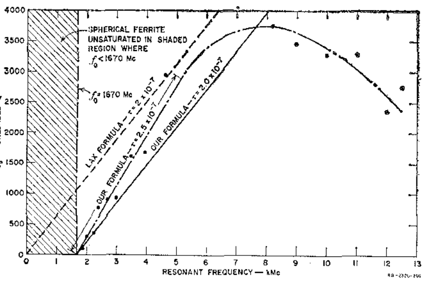

Fig. 1.

It is possible to reinterpret Lax's susceptibility formula so that it now becomes the same as the new formula. This is done by substituting for τ in Lax's equation a new relaxation time $(\omega_0 - N_z\omega_m)\tau/\omega_0$, where N_z is the z-demagnetizing factor. In the case of the sphere, $N_z = \frac{1}{3}$. However, the new formula is obtained straightforwardly from the Bloch-Bloembergen equation of motion, and the equivalent circuit interpretation, without the artificial introduction of a relaxation time which in turn depends on a demagnetizing factor.

Measurements were made of the Q_u of a highly polished spherical single crystal of yttrium-iron-garnet, using the method described by Ginzton.[6] The yttrium-iron-garnet sphere was mounted in a short-circuited waveguide or transmission line near the short circuited end. A 0.064-inch diameter single crystal yttrium-iron-garnet sphere was used in these measurements.

The experimental values of Q_u are shown as points in Fig. 1. An approximate fit to these data is given by the "dash-dot" curve. The lower frequency portion of this experimental curve between 1.67 kMc and about 5 kMc is a straight line which can be represented by the new formula, assuming $\tau = 2.5 \times 10^{-7}$. In this low frequency region at least, the data appear to support the new formula for Q_u. At higher frequencies the experimental curve for Q_u flattens off and, above about 8 kMc, Q_u decreases with increasing frequency.

It is planned to publish a complete analysis and discussion of these and other related data in the near future.

P. S. CARTER, JR.
C. FLAMMER
Stanford Res. Inst.
Menlo Park, Calif.

[6] Edward L. Ginzton, "Microwave Measurements," in "Microwave Measurements," McGraw-Hill Book Co., Inc., New York, N. Y., ch. 9, pp. 391–434; 1957.

A Note on the Derivation of the Fields in a Radial Line*

The concept of a radial transmission line is frequently used in the description of such devices as cylindrical cavity resonators and horn radiators. An approach[1–3] to the problem of determining the electric and magnetic fields in the radial line has been to solve Maxwell's equations in component form with appropriate boundary conditions. While the following derivation yields nothing new, it does, however, have the advantages of being simple and of requiring a minimum of guess work as compared to other methods of solving this problem.

The technique employed here is based on the fact[4] that the general solution of the vector Helmholtz equation

$$\nabla^2 \bar{A}(\bar{r}) + k^2 \bar{A}(\bar{r}) = 0 \tag{1}$$

consists of a linear combination of three vector functions generated in turn from three scalar functions:

$$\bar{L}(\bar{r}) = \nabla\phi(\bar{r})$$
$$\bar{M}(\bar{r}) = \nabla \times [\bar{u}\psi(\bar{r})]$$
$$\bar{N}(\bar{r}) = \frac{1}{k}\nabla \times \nabla \times [\bar{u}\chi(\bar{r})].$$

The vector $\bar{u}$ is a constant vector and ϕ, ψ and χ are each solutions of the scalar Helmholtz equation; *e.g.*, $\nabla^2\phi(\bar{r}) + k^2\phi(\bar{r}) = 0$.

Consider the geometry shown in Fig. 1. The region of interest is the semi-infinite space between the perfectly conducting, parallel bounding surfaces at $z=0$ and $z=b$. Assume that the fields have a time dependence of the form $e^{j\omega t}$ and that no free charge exists in the region between the bounding surfaces. Subject to these conditions, the electric and magnetic fields in the region $0 \le z \le b$ must satisfy an equation of the same form as (1) with $k^2 = -\gamma_0^2 = \omega^2\mu\epsilon[1 - j(\sigma/\omega\epsilon)]$ where σ, ϵ and μ are respectively the conductivity, permittivity and permeability of the medium between the surfaces and ω is the radian frequency.

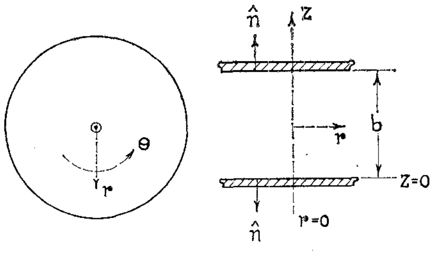

Fig. 1—A radial transmission line consisting of two parallel conducting planes.

Because of the manner in which they are defined, $\bar{M}$ and $\bar{N}$ are solenoidal as are $\bar{E}$ and $\bar{H}$ in this case, and it follows that the $\bar{M}$ and $\bar{N}$ solutions for (1) could correspond to either the electric or the magnetic field depending upon the choice of boundary conditions at $z=0$ and $z=b$.

As an illustration let us require that $\bar{M}$ and $\bar{N}$ satisfy the boundary conditions for the electric field, namely, $\hat{n}\times\bar{M} = \hat{n}\times\bar{N} = 0$. Writing the $\bar{M}$ solution in terms of the unit vector in the z-direction, $\bar{M} = \nabla\times[\bar{u}_z\psi(r,\theta,z)]$, and applying the boundary conditions after solving the scalar Helmholtz equation by the standard approach of separating variables leads to

$$\bar{E}_{m,n} = \bar{M}_{m,n} = \nabla \times \left\{\bar{u}_z[K_1 J_m(\beta r) + K_2 Y_m(\beta r)]e^{\pm jm\theta}\sin\left(\frac{n\pi}{b}z\right)\right\}$$
$$m, n = 0, 1, 2 \cdots. \tag{2}$$

K_1 and K_2 are arbitrary constants which specify the amplitude of the field. J_m and Y_m are the Bessel functions of the first and second kind respectively and $\beta^2 = -\gamma_0^2 - (n\pi/b)^2$. In this case, K_2 must be equal to zero because of the singularity of $Y_m(\beta r)$ at $r=0$, but if the region of interest is that for which $r \ge r_0 \ne 0$, then K_2 need not be zero. The corresponding magnetic field can be found from

$$\nabla \times \bar{E}_{m,n} = -j\omega\mu\bar{H}_{m,n}. \tag{3}$$

* Received by the PGMTT, June 10, 1960. This work was supported in part by the U. S. Army Signal Engrg. Labs., Fort Monmouth, N. J., under Contract DA 36-039 sc 78254.

[1] S. A. Schelkunoff, "Electromagnetic Waves," D. Van Nostrand Co., Inc., New York, N. Y., pp. 260–275; 1943.

[2] H. R. L. Lamont, "Wave Guides," Methuen and Co. Ltd., London, Eng., pp. 19–23; 1942.

[3] C. G. Montgomery, R. H. Dicke, and E. M. Purcell, "Principles of Microwave Circuits," McGraw-Hill Book Co., Inc., New York, N. Y., pp. 252–254; 1948.

[4] P. M. Morse and H. Feshbach, "Methods of Theoretical Physics," McGraw-Hill Book Co., Inc., New York, N. Y. pp. 1764–1767; 1953.

The fields obtained from (2) and (3) are the so-called "transverse" electric fields since $E_z(m, n)$ vanishes.

Following an identical procedure, the $\overline{N}$ solution leads to

$$E'_{m,n} = \overline{N}_{m,n} = -\frac{j}{\gamma_0}\nabla \times \nabla \times \left\{\hat{u}_z[K_3 J_m(\beta r) + K_4 Y_m(\beta r)]e^{\pm jm\theta} \cos\left(\frac{n\pi}{b} z\right)\right\}$$

$$m, n = 0, 1, 2 \cdots. \quad (4)$$

Again the corresponding magnetic field, $\overline{H'}_{m,n}$, can be found using (3). These fields are the so-called "transverse" magnetic fields since $H'_{z(m,n)} = 0$.

It is also possible to derive the magnetic fields from the $\overline{M}$ and $\overline{N}$ solutions by requiring that $\hat{n}\cdot\overline{M} = \hat{n}\cdot\overline{N} = 0$ at $z=0$ and $z=b$, and then use (3) to determine the components of the electric fields.

JOSEPH F. DIENST
Microwave Electronics Lab.
College of Engrg.
Rutgers, the State University
New Brunswick, N. J.

Surface Waves on Symmetrical Three-Layer Sandwiches*

The theory of surface waves on plane dielectric slabs has been presented by Plummer and Hansen.[1] Additional numerical results are shown in Figs. 1 and 2 for the lowest order TM and TE modes that can exist on a grounded dielectric slab. The slab has thickness d_s, and a relative dielectric constant of 4. It is separated by an air gap of thickness a from the ground plane. c/v represents the ratio of the velocity of light in free space and the phase velocity of the surface wave. By image theory, these modes (TM_0 and TE_1) can also exist on a symmetrical, three-layer, air-core sandwich to which the given numerical data also apply.

Figs. 3 and 4 show similar data for the TM_1 and TE_0 modes. These modes disappear if a ground plane is inserted at the center of the sandwich. For this reason, these modes are usually ignored in the literature.

The fields of a surface wave decay as $e^{-\alpha x}$, with distance from the surface of the plane structure. The attenuation constant α, is not independent but is directly related to the phase velocity by $(\alpha\lambda_0)^2 = 4\pi^2[(c/v)^2 - 1]$, as shown in Fig. 5. This may be called a universal curve of $\alpha\lambda_0$ vs c/v, because it applies to TE and TM modes on any lossless plane structure.

The results mentioned were obtained under a project sponsored by the Air Research and Development Command, USAF.

J. H. RICHMOND
Antenna Lab.
The Ohio State University
Columbus, Ohio

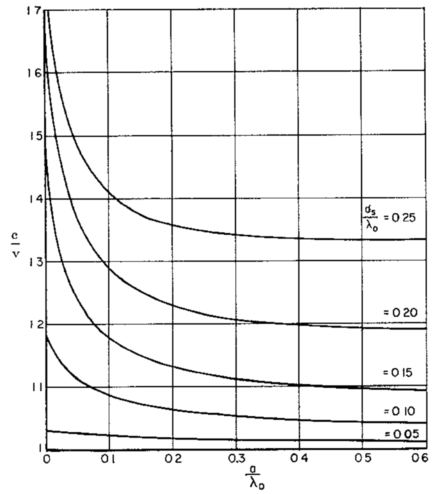

Fig. 1—Phase velocity ratio vs core thickness for the TM_0 mode on an air-core sandwich. (Data also apply to a single slab over a ground plane, with an air space.)

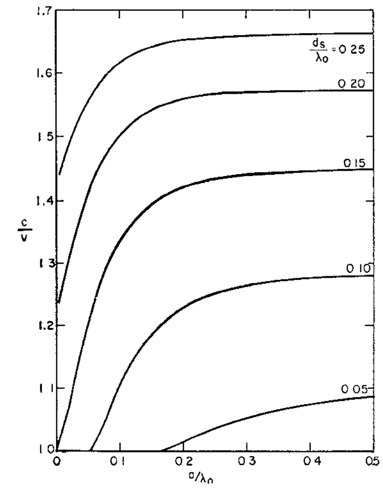

Fig. 2—Phase velocity ratio vs core thickness for the TE_1 mode on an air-core sandwich. (Data also apply to a single slab over a ground plane, with an air space.)

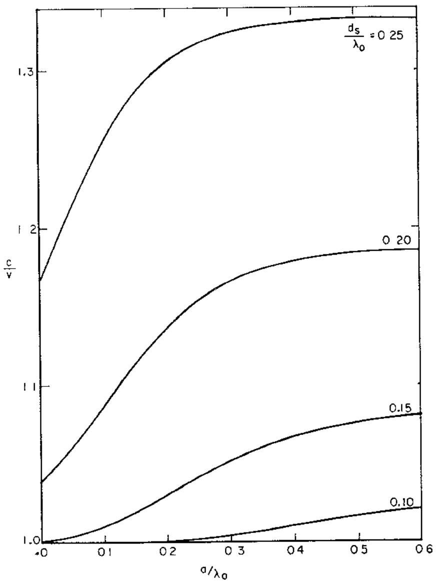

Fig. 3—Phase velocity ratio vs core thickness for the TM_1 mode on an air-core sandwich.

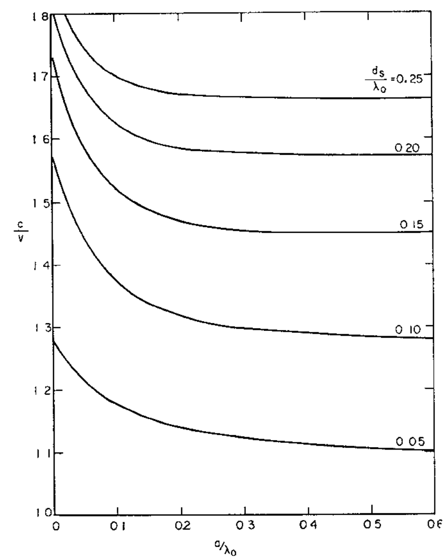

Fig. 4—Phase velocity ratio vs core thickness for the TE_0 mode on an air-core sandwich.

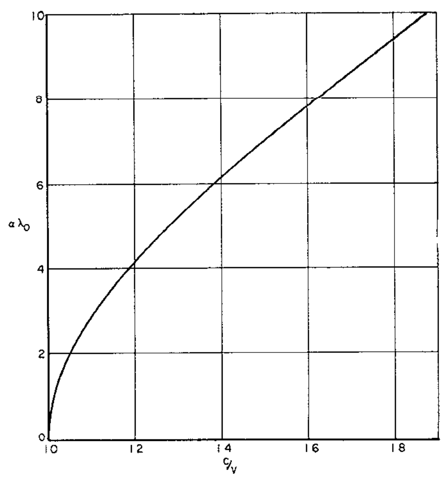

Fig. 5—Universal curve of $\alpha\lambda_0$ vs c/v.

* Received by the PGMTT, June 20, 1960.

[1] R. Plummer and R. Hansen, *Proc. IEE*, pt. C, mono. 238R; May, 1957.